



Colloidal Plasmonic Titanium Nitride Nanoparticles: Properties and Applications

Guler, Urcan; Suslov, Sergey; Kildishev, Alexander V.; Boltasseva, Alexandra; Shalaev, Vladimir M.

Published in:
Nanophotonics

Link to article, DOI:
[10.1515/nanoph-2015-0017](https://doi.org/10.1515/nanoph-2015-0017)

Publication date:
2015

Document Version
Publisher's PDF, also known as Version of record

[Link back to DTU Orbit](#)

Citation (APA):
Guler, U., Suslov, S., Kildishev, A. V., Boltasseva, A., & Shalaev, V. M. (2015). Colloidal Plasmonic Titanium Nitride Nanoparticles: Properties and Applications. *Nanophotonics*, 4(1), 269-276.
<https://doi.org/10.1515/nanoph-2015-0017>

General rights

Copyright and moral rights for the publications made accessible in the public portal are retained by the authors and/or other copyright owners and it is a condition of accessing publications that users recognise and abide by the legal requirements associated with these rights.

- Users may download and print one copy of any publication from the public portal for the purpose of private study or research.
- You may not further distribute the material or use it for any profit-making activity or commercial gain
- You may freely distribute the URL identifying the publication in the public portal

If you believe that this document breaches copyright please contact us providing details, and we will remove access to the work immediately and investigate your claim.

Research Article

Open Access

Urcan Guler, Sergey Suslov, Alexander V. Kildishev, Alexandra Boltasseva, and Vladimir M. Shalaev*

Colloidal Plasmonic Titanium Nitride Nanoparticles: Properties and Applications

DOI 10.1515/nanoph-2015-0017

Received October 28, 2014; accepted June 21, 2015

Abstract: Optical properties of colloidal plasmonic titanium nitride nanoparticles are examined with an eye on their photothermal and photocatalytic applications via transmission electron microscopy and optical transmittance measurements. Single crystal titanium nitride cubic nanoparticles with an average size of 50 nm, which was found to be the optimum size for cellular uptake with gold nanoparticles [1], exhibit plasmon resonance in the biological transparency window and demonstrate a high absorption efficiency. A self-passivating native oxide at the surface of the nanoparticles provides an additional degree of freedom for surface functionalization. The titanium oxide shell surrounding the plasmonic core can create new opportunities for photocatalytic applications.

Keywords: refractory plasmonics; plasmonic heating; photothermal effect; photodynamic therapy; hot electrons; photocatalysis

Materials research has been the backbone in the field of plasmonics for the last few years. Unique properties supplied by alternative plasmonic materials have created

an excitement to develop technologies for a broad range of applications. The wide range of carrier concentrations available from several material classes spans the electromagnetic spectrum from the ultra-violet through the mid-infrared [2]. Additionally, the broad variety of materials studied in the field provide extra degrees of freedom to solve technological challenges thanks to the unique properties such as tunability, process compatibility, chemical stability, etc [3].

Transition metal nitrides, especially titanium nitride (TiN), have been studied for the last three decades due to the unique combination of their material properties [4]. Metallic behavior of TiN combined with its hardness and chemical stability has attracted attention in microelectronics research [5]. Adjustable optical properties and stoichiometry of TiN thin films were examined in the 1990s [6]. The optical characterization of TiN thin films was extensively performed later with the increasing interest in the field of plasmonics [7–10]. Improved properties with epitaxial TiN thin films have recently been demonstrated with a hyperbolic metamaterial and a plasmonic waveguide [11, 12]. As a refractory plasmonic material, TiN holds the potential to solve critical issues associated with the softness and low melting points of plasmonic metals such as gold and silver [13, 14]. In contrast to thin films, TiN nanoparticles have not been extensively studied until recently. Localized surface plasmons (LSPs) in TiN nanoparticles were first theoretically analyzed by Quinten [15], while their first experimental demonstration was performed by Reinholdt et al. [16]. In their work, cubic nanoparticles smaller than 10 nm with a broad size dispersion were fabricated through laser ablation, and plasmon resonance peaks centered around 730 nm wavelength were reported. Reinholdt et al. proposed the use of TiN nanoparticles as inorganic, stable color pigments. We have previously shown that TiN nanoparticles provide field enhancement comparable to that achievable with Au, with a broader peak spectrally positioned in the biological transparency window [17]. In a more recent study, we experimentally analyzed the absorption efficiencies of lithographically fabricated TiN and Au nanoparticles and showed that TiN nanoparticles can

Urcan Guler, Alexander V. Kildishev: School of Electrical & Computer Engineering and Birck Nanotechnology Center, Purdue University, West Lafayette, IN 47907, USA; Nano-Meta Technologies Inc., 1281 Win Henschel Boulevard, West Lafayette, IN 47906, USA

Sergey Suslov: Birck Nanotechnology Center, Purdue University, West Lafayette, IN 47907, USA

Alexandra Boltasseva: School of Electrical & Computer Engineering and Birck Nanotechnology Center, Purdue University, West Lafayette, IN 47907, USA; Nano-Meta Technologies Inc., 1281 Win Henschel Boulevard, West Lafayette, IN 47906, USA; DTU Fotonik, Department of Photonics Engineering, Technical University of Denmark, Lyngby, DK-2800, Denmark

***Corresponding Author: Vladimir M. Shalaev:** School of Electrical & Computer Engineering and Birck Nanotechnology Center, Purdue University, West Lafayette, IN 47907, USA; Nano-Meta Technologies Inc., 1281 Win Henschel Boulevard, West Lafayette, IN 47906, USA; Email: shalaev@purdue.edu.



© 2015 V. M. Shalaev et al., licensee De Gruyter Open.

This work is licensed under the Creative Commons Attribution-NonCommercial-NoDerivs 3.0 License.

Brought to you by | DTU - Technical Information Center of Denmark (DTIC)

Authenticated

Download Date | 11/25/15 11:55 AM

provide enhanced local heating in the biological transparency window when compared to identical Au samples [18].

As a refractory plasmonic material, TiN delivers chemical stability at elevated temperatures. The high melting point and hardness of the material enables the use of plasmonic effects for applications where tough operational conditions are required [13, 14, 19, 20]. Heat assisted magnetic recording [21], solar/thermophotovoltaics [22], plasmon enhanced photocatalysis [23–25], and plasmon assisted chemical vapor deposition [26] are some of the applications that could take advantage of durable plasmonic TiN nanostructures. TiN is a chemically inert material widely used in CMOS and biomedical devices [5, 27–30]. Combined with the localized surface plasmon resonance (LSPR) peak located in the biological transparency window [17], bio-compatibility of the material makes it a promising alternative for plasmonic photothermal therapy [18]. Consequently, the plasmonic properties of TiN colloidal nanoparticles are clearly important for future studies on the feasibility of the material for therapeutic applications. In this Letter, we examine the optical properties of aqueous TiN nanoparticle solution and show that the dipolar resonance matches well with the biological transparency window, suppressing the need for large nanoparticles and relatively complex systems of conventional metals that have been used so far. Transmission electron microscope (TEM) studies show that TiN nanoparticles are single crystalline with lattice constants in agreement with the literature values. The observed optical properties of TiN nanoparticles are of the same quality as those of the epitaxial thin films grown on c-sapphire substrates reported recently [18]. A thin native oxide layer, which can be removed or thickened at will [31, 32], is observed at the surface of TiN nanoparticles. Surface oxide is a self-passivating layer with a thickness of 1–2 nm. The presence of a thin oxide layer could provide an additional degree of freedom for surface chemistry studies. Extensively studied oxide chemistry could be useful for surface functionalization where the inertness of TiN could be a problem. These results reveal the high potential of TiN as a plasmonic material for photothermal therapy. Further work is required in order to test the bio-compatibility and stability of nanoparticles as well as clearance from the body after treatment. The surface chemistry of TiN colloidal nanoparticles, with or without the native oxide layer, is an interesting research area. Plasmonic TiN nanoparticles with an oxide shell are particularly interesting for plasmon-induced photocatalysis [23].

The enhanced absorption properties of plasmonic nanoparticles are desired for applications such as plas-

monic photothermal therapy where local heating is required. Nanoparticles can be delivered into a tumor region selectively, and a confined volume around the plasmonic nanoparticle can be efficiently heated via laser illumination at resonance wavelengths [33]. The accumulation of the nanoparticles and their selective heating results in the ablation of the tumor while damage to healthy tissue is kept minimal [33, 34]. One of the fundamental limitations of the method is the small penetration depth of light through biological tissue, usually on the order of a few centimeters. The near infrared region of the electromagnetic spectrum is known as the biological transparency window due to the reduced absorption of light in the region between wavelengths 700 nm and 1000 nm, enabling deeper penetration and more efficient power delivery to the region of interest. Thus, it is of high importance to design nanoparticles with plasmonic resonances in the biological transparency window. Gold has been the primary material for use in plasmonic photothermal therapy due to several factors. Bio-compatibility, high plasmonic performance and well-studied surface chemistry are among the top reasons for the frequent use of Au. However, the dipolar LSPR peak obtained from a small Au nanoparticle is located around a wavelength of 550 nm, which is away from the biological transparency window. This spectral mismatch problem can be solved by using nanoparticles with relatively larger sizes, or engineered geometries. Hirsch et al. demonstrated a smart solution by using Au nanoshells in order to achieve plasmonic resonance in the biological transparency window at the expense of relatively large particle sizes exceeding 100 nm [35, 36]. However, the large size leads to additional complications such as limited cellular uptake and more difficult clearance from the body. It has been shown that cellular uptake is more efficient for nanoparticle sizes around 50 nm [1]. Biodegradable structures were recently suggested as a solution to the clearance problem [37]. In their work, Huang et al. demonstrated the use of closely packed 26 nm Au nanoparticles, with a total cluster size of 200 nm, as plasmonic antennas for photothermal therapy and reported improved clearance (most likely due to the dissociation of the nanoparticle assemblies after laser irradiation). However, this concrete step toward the improved clearance brings new questions such as the stability of the nanoparticle assembly and controllability of the biodegradation process. In another recent study, Goodman et al. reported the instability of hollow Au-Ag nanoshells, which provide shell structures with dimensions smaller than 100 nm, during *in-vivo* applications [38]. Another approach to red-shift the plasmonic resonance is to engineer the nanoparticle aspect ratio. Gold nanorods can be used as simpler geometry parti-

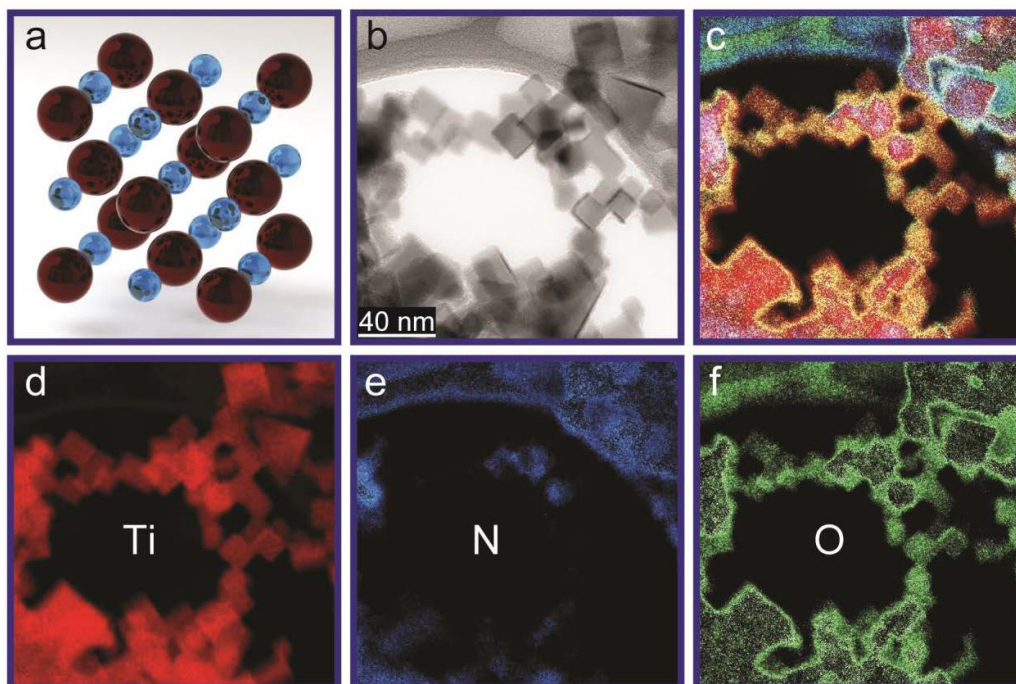


Figure 1: (a) Illustration of a rock salt TiN crystal unit cell. (b) TEM image of TiN nanoparticles with dominant cubic shapes following the rock salt lattice. (c) Combined elemental map of the same sample region. (d–f) Individual elemental maps of Ti, N and O, respectively. The self-passivating native oxide layer at the surface of the nanoparticles is distinct with a 1–2 nm thickness.

cles for theranostics [39]. However, surfactants originating from the synthesis of the particle and suppressed cellular uptake due to the increased aspect ratio are the problems that need to be addressed [1, 40, 41]. Carbon nanotubes exhibit a broad absorption band in the near infrared region making them interesting for photothermal therapy; however, compared with plasmonic nanoparticles, absorption efficiencies are relatively low [33].

Titanium nitride exhibits optical properties similar to those of Au and has dielectric permittivity zero crossover in the visible wavelength range, making it plasmonic in this spectral region. Previously we have calculated that the scattering efficiencies of spherical TiN nanoparticles are comparable with those achieved in Au nanoparticles, and the dipolar peak of TiN is positioned in the near infrared region making it promising for theranostic applications [17]. Recently, the experimental verification of the higher absorption efficiencies obtained from lithographically fabricated TiN nanoparticles compared with identical Au structures were reported [18]. Combined with the bio-compatibility of TiN, high absorption efficiency of simple-geometry nanoparticles is of high interest [29]. Titanium nitride nanoparticles in powder form can be fabricated by using nitridation of Ti or TiO_2 at high temperatures, laser ablation of Ti or TiN targets, mechanical alloying, microwave plasma technique, vapor synthesis,

reduction-nitridation, and other techniques [16, 31, 42–48]. In this work, aqueous solutions are prepared with commercially available TiN powders (PlasmaChem) with an average nanoparticle size of 50 nm. Optical transmittance measurements from aqueous solutions are performed with a Lambda 950 Vis/NIR Spectrophotometer (Perkin Elmer). Nanoparticle size distribution is determined by dynamic light scattering technique with a Zetasizer (Malvern Instruments). FEI Titan 80/300 Environmental TEM equipped with a Tridiem 863 Gatan Imaging Filter is used for electron microscopy. Samples for TEM characterization are prepared on Lacey Carbon Films (Ted Pella) to avoid substrate signal.

Energy filtered TEM images of TiN nanoparticles dispersed on a Lacey Carbon membrane are presented in Figure 1. The electron beam passing through the nanoparticle sample experiences energy losses unique to the elements in the sample. Subsequent to traversing the sample, the electron beam is dispersed through a magnetic prism and specific energy windows are selected with an energy slit. Filtered electrons, with the energy loss characteristic to a particular element, can be used to form an image of the element of interest [49]. We investigate the distribution of nitrogen (N), titanium (Ti) and oxygen (O) in TiN nanoparticles with a slit width of 5 eV located around the energies 401, 456 and 532 eV, respectively. Figure 1(a–b) shows the

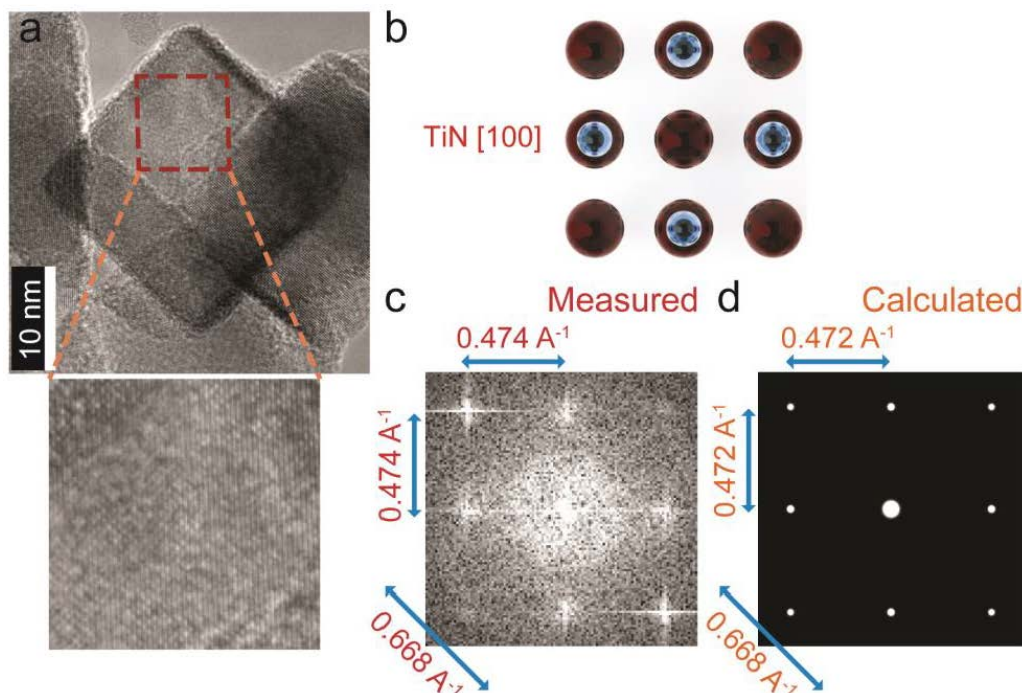


Figure 2: (a) HRTEM image of a single cubic TiN nanoparticle. The inset shows magnified image of the region designated with dashed rectangle. (b) The unit cell of rock salt TiN crystal with [100] lattice vector pointing out of the page plane. (c) FFT diffractogram of the designated region taken from the HRTEM image. (d) Calculated FFT pattern from tabulated data [53]. Measured lattice constant, 4.22 Å, is in good agreement with tabulated bulk value, 4.24 Å.

unit cell of a rock salt TiN crystal and a TEM image of the sample under test, respectively. The most stable form of TiN, cubic shape [16, 50], is evident from the image. Figure 1(c) shows the combined image of the elemental maps, while Figure 1(d-f) shows the maps of each element under investigation. The presence of Ti and N is clear from the images. A native oxide is also observed on the surface of the nanoparticles. In accordance with the literature, the thickness of the oxide at room temperature is around 1–2 nm. The presence of the native oxide layer is of particular importance. First of all, if the oxide layer is not desired, it can be removed by nitridation at elevated temperatures [31]. On the other hand, we find it particularly important to have an oxide layer since the chemical inertness of TiN could be a potential problem for surface chemistry studies. A thin oxide layer at the surface of the nanoparticles could be used as an additional degree of freedom for surface modifications. In fact, the wide use of titanium oxides as a pigment in food and personal care products resulted in intensive research on the chemistry of nanometer scale particles [51]. Well-established chemistry of titanium oxide nanoparticles would be useful for surface functionalization and particle dispersion of oxide coated TiN nanoparticles. Additionally, the thickness of the oxide layer could

be controllably increased at elevated temperatures, if desired [52].

Oxide-coated TiN nanoparticles can also be used for plasmon-induced hot carrier generation for photocatalytic applications such as water splitting [23]. A plasmonic core with high absorption efficiency, TiN, coated with an efficient photocatalyst, TiO₂, has a significant potential for this newly developing area.

The optical properties of TiN vary significantly depending on the stoichiometry and crystallinity of the structure. Single crystalline nanoparticles with minimal defects are desired for better oscillator quality and plasmonic performance. Figure 2 shows high-resolution TEM (HRTEM) images of a TiN nanoparticle, which reveals the cubic shape of the nanoparticle as well as the lattice planes. The thin oxide layer at the surface of the nanoparticle can be noticed from the HRTEM image as well. Figure 2(b) is the illustration of the rocksalt structure with [100] lattice vector pointing out of the page plane. A fast Fourier transform (FFT) diffractogram obtained from the region shown in the inset is given in Figure 2(c). Figure 2(d) shows the simulated FFT diffractogram with the constants taken from the tabulated data [53]. The lattice constant of an individual nanoparticle is measured to be 4.22 Å, which is very close to the tabulated bulk value of 4.24 Å. Based on the ex-

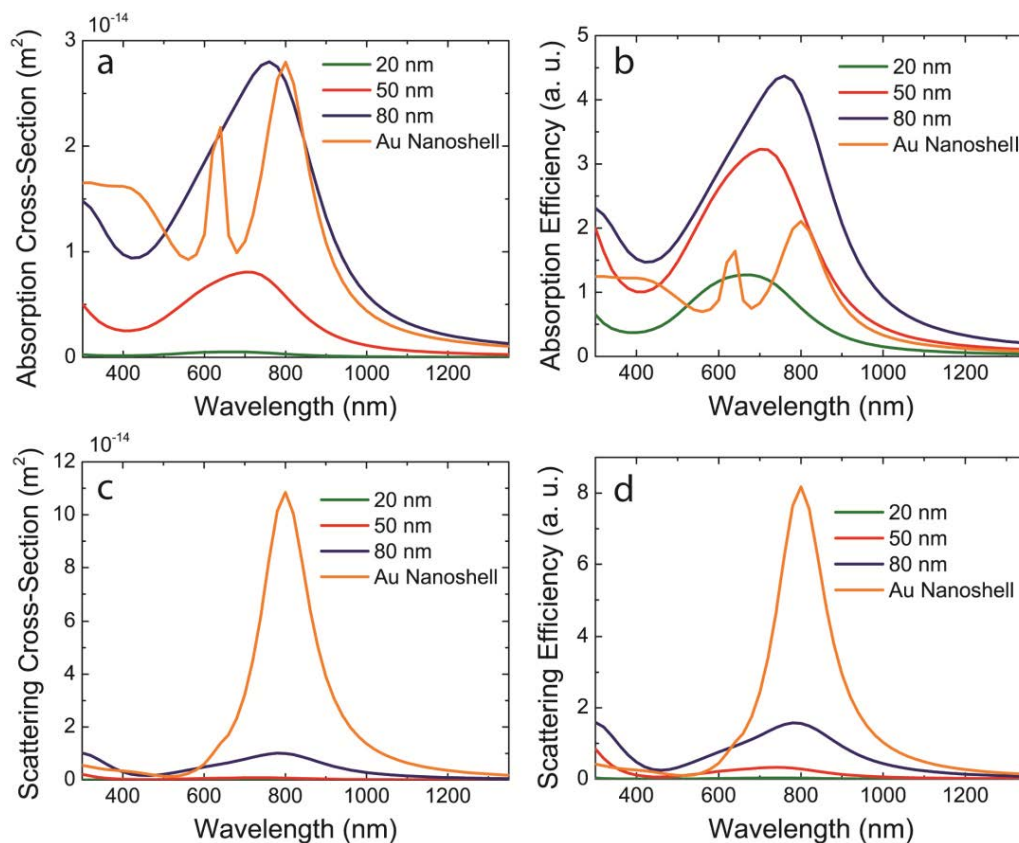


Figure 3: (a) Calculated absorption cross-section of TiN nanoparticles with sizes of 20, 50 and 80 nm compared to Au nanoshell with inner and outer diameters of 110 and 130 nm, respectively. (b) Absorption efficiencies of the same nanoparticles. Higher efficiencies in the biological transparency window obtained with smaller TiN nanoparticles would resolve problems arising from larger sizes of Au nanoshells. (c-d) Scattering cross-section and efficiencies of the same nanoparticles. Au nanoshell provides higher scattering efficiencies due to a larger particle size and more metallic behavior of the material. Efficiencies are calculated as optical cross-sections normalized by geometric cross-sections [55].

perimental results showing the high crystalline quality of nanoparticles, we use a dielectric permittivity measured from lattice-matched, single crystalline TiN thin films in our simulations in this work [18].

It has been demonstrated that lithographically fabricated TiN nanoparticles are efficient plasmonic absorbers in the biological transparency window [18]. However, lithographic nanostructures deposited under optimized growth conditions have limited use in biological applications and colloidal TiN nanoparticles with similar plasmonic quality are essential for applications such as photothermal treatment. Among several materials with high plasmonic performance, we choose Au as the reference material due to its chemical stability and biocompatibility. Due to their well demonstrated success in biological applications, we use nanoshell structures in order to compare the performance of colloidal TiN nanoparticles. Figure 3 shows the absorption cross-sections and efficiencies of TiN nanoparticles with sizes of 20, 50

and 80 nm. Gold nanoshells designed for resonance in the bio-transparency window are included as a reference. The inner and outer radii of the nanoshells were chosen to be 55 and 65 nm as these parameters are widely used in photothermal treatment [35]. Figure 3(a) shows that absorption cross-sections comparable to Au nanoshells can be obtained with TiN nanoparticles of much smaller dimensions. For example, 80 nm TiN particles provide the same absorption cross-section peak with a volume 2.25 times less and cross-sectional area 2.07 times smaller than the nanoshell. 50 nm particles, providing approximately one third of the absorption cross-section, are 9.2 times smaller in volume and 5.3 times smaller in the cross-sectional area. As a result, the absorption efficiencies of TiN nanoparticles given in Figure 3(b) exceed the efficiency of the reference nanoshell. 50 nm particles, which are found to have the optimum dimensions for efficient cellular uptake in the case of Au [1], provide 50% better absorption efficiency when the peak positions are comparable and have slightly

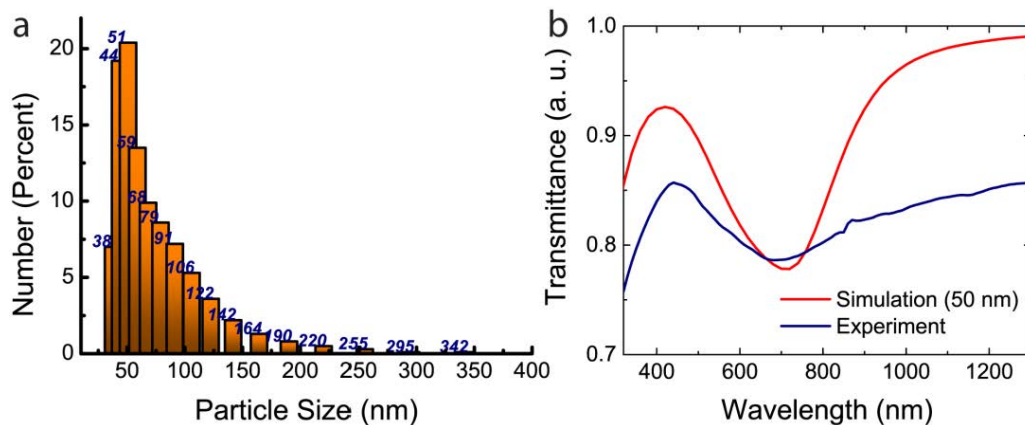


Figure 4: Dynamic light scattering measurement of the size dispersion for colloidal plasmonic TiN nanoparticles. Peak value around 50 nm is a desired size for more efficient cellular uptake. The long tail with marginal large dimensions is likely due to clustering effects. (b) Transmittance data taken from aqueous TiN sample (blue) and calculated data for mono-sized 50 nm nanoparticle solution (red). Calculated transmittance with mono-sized nanoparticle solution agrees well on the peak spectral position and amplitude with the experimental data. Broader experimental peak can be attributed to the size dispersion as observed in dynamic light scattering measurement.

better efficiency at 800 nm wavelength. The broader resonance peak obtained from TiN nanoparticles is another advantage that relaxes the restrictions on particle size dispersion. It should be noted that smaller nanoparticle dimensions are desirable due to many critical requirements including efficient cellular uptake and clearance of particles after treatment [1, 37, 38].

Scattering efficiency of TiN nanoparticles, on the other hand, is not superior to Au nanoshell. Here, the main reason is the significant size difference which favors scattering from a larger nanostructure [54]. It has also been shown that TiN nanoparticles are relatively deficient scatterers compared to identical structures made of Au [17]. Figure 3(c) shows the scattering cross-section of TiN nanoparticles and Au nanoshells where a significant difference can be observed. The difference in the scattering efficiencies given in Figure 3(d) is reduced, but the TiN peak values are still not comparable to those of Au nanoshells. Consequently, the use of TiN nanoparticles for local heating applications such as photothermal therapy and drug delivery seem very possible, applications based on the near-field enhancement would require careful optimization.

We use optical transmittance data as an evidence of the plasmonic properties of colloidal TiN nanoparticles. The assumption that the dielectric permittivity of TiN nanoparticles are similar to that of the epitaxially grown thin films can also be checked by comparing experimental data and simulations. Figure 4(a) shows the size dispersion of colloidal TiN nanoparticles dispersed in water. Dynamic light scattering reveals that the majority of the nanoparticles are smaller than 100 nm with a peak around

50 nm and a tail extends up to a few hundred nanometers that is likely due to clustering and marginal number of large nanoparticles. With a peak around 50 nm and shape aspect ratio of 1, the sample is promising for efficient cellular uptake [1], but needs further investigations. Figure 4(b) shows the transmittance data of the sample along with the simulations of the aqueous solution consisting of mono-sized 50 nm particles. Experimental data with a transmittance dip around 700 nm agrees well with the simulation results presented in previous and the current work. Calculated transmittance data for a mono-sized sample exhibits a narrower peak with very accurate amplitude, verifying the accuracy of the assumption that nanoparticles are single crystalline with high purity. The deviation in the width of the peak is likely due to the broad size dispersion of the colloidal sample and clustering effects. It is anticipated that future development of TiN synthesis and surface chemistry will uncover better control of size dispersion.

Here, we present results of an initial study on plasmonic TiN colloidal nanoparticles with a focus on photothermal therapy and local heating applications as well as potential use in water splitting. The results show that plasmonic TiN colloidal samples hold enormous potential, hence require further studies involving the biocompatibility at nanoscale, surface chemistry, cellular uptake efficiency, and size dispersion control.

In conclusion, colloidal TiN nanoparticles exhibit plasmonic properties in the visible region and mimic the optical properties of recently developed crystalline TiN thin films. 50 nm particles provide absorption efficiencies better than larger Au nanoshell structures, leading to

the opportunity of using smaller and simpler plasmonic nanoparticles for photothermal therapies. A thin native oxide shell formed on TiN structures is likely to provide an additional degree of freedom for surface functionalization of the nanoparticles. Plasmonic titanium nitride core covered with a titanium oxide shell is also a promising path to a more efficient plasmon-induced photocatalysis.

Acknowledgement: We would like to thank Dr. Gururaj Naik for fruitful discussions and Nathaniel Kinsey for help in preparation of this manuscript. The authors acknowledge support from the following grants: ONR-MURI grant N00014-10-1-0942, ARO grant 57981-PH (W911NF-11-1-0359) and NSF MRSEC grant DMR-1120923.

Note: The authors declare no competing financial interest.

References

- [1] Chithrani B.D., Ghazani A.A., Chan W.C.W., Determining the Size and Shape Dependence of Gold Nanoparticle Uptake into Mammalian Cells, *Nano Letters*. 2006, 2006/04/01, 6(4): 662–8.
- [2] Boltasseva A., Atwater H.A., Materials science. Low-loss plasmonic metamaterials, *Science* 2011, 331(6015): 290–1.
- [3] Naik G.V., Shalaev V.M., Boltasseva A., Alternative plasmonic materials: beyond gold and silver, *Adv Mater.* 2013; 25(24): 3264–94.
- [4] Wittmer M., Properties and microelectronic applications of thin films of refractory metal nitrides, *Journal of Vacuum Science & Technology A: Vacuum, Surfaces, and Films* 1985, 3(4): 1797–803.
- [5] Tang T.E., Che-Chia W., Haken R.A., Holloway T.C., Hite L.R., Blake T.G.W., Titanium nitride local interconnect technology for VLSI, *Electron Devices, IEEE Transactions on*. 1987, 34(3): 682–8.
- [6] Tompkins H.G., Gregory R., Boeck B., Optical properties of titanium nitride thin films, *Surface and Interface Analysis* 1991, 17(1): 22–4.
- [7] Steinmüller-Nethl D., Kovacs R., Gornik E., Rödhammer P., Excitation of surface plasmons on titanium nitride films: determination of the dielectric function, *Thin Solid Films* 1994, 237(1): 277–81.
- [8] Hibbins A.P., Sambles J.R., Lawrence C.R., Surface plasmon-polariton study of the optical dielectric function of titanium nitride, *Journal of Modern Optics* 1998, 45(10): 2051–62.
- [9] Chen N.C., Lien W.C., Liu C.R., Huang Y.L., Lin Y.R., Chou C., et al., Excitation of surface plasma wave at TiN/air interface in the Kretschmann geometry, *Journal of Applied Physics* 2011, 109(4): 043104–7.
- [10] Naik G.V., Schroeder J.L., Ni X., Kildishev A.V., Sands T.D., Boltasseva A., Titanium nitride as a plasmonic material for visible and near-infrared wavelengths, *Optical Materials Express* 2012, 2(4): 478–89.
- [11] Naik G.V., Saha B., Liu J., Saber S.M., Stach E.A., Irudayaraj J.M.K., et al., Epitaxial superlattices with titanium nitride as a plasmonic component for optical hyperbolic metamaterials, *Proceedings of the National Academy of Sciences* 2014 May 12, 2014.
- [12] Kinsey N., Ferrera M., Naik G.V., Babicheva V.E., Shalaev V.M., Boltasseva A., Experimental demonstration of titanium nitride plasmonic interconnects, *Optics Express* 2014 2014/05/19, 22(10): 12238–47.
- [13] Guler U., Boltasseva A., Shalaev V.M., Refractory Plasmonics, *Science* 2014, 344(6181): 263–4.
- [14] Guler U., Shalaev V.M., Boltasseva A., Nanoparticle plasmonics: going practical with transition metal nitrides, *Materials Today* 2015, 18(4): 227–37.
- [15] Quinten M., The color of finely dispersed nanoparticles, *Applied Physics B*. 2001, 2001/09/01, 73(4): 317–26.
- [16] Reinholdt A., Pecenkova R., Pinchuk A., Runte S., Stepanov A.L., Weirich T.E., et al., Structural, compositional, optical and colorimetric characterization of TiN-nanoparticles; *The European Physical Journal D - Atomic, Molecular, Optical and Plasma Physics* 2004, 2004/10/01, 31(1): 69–76.
- [17] Guler U., Naik G.V., Boltasseva A., Shalaev V.M., Kildishev A.V., Performance analysis of nitride alternative plasmonic materials for localized surface plasmon applications, *Applied Physics B*. 2012, 2012/05/01, 107(2): 285–91.
- [18] Guler U., Ndukaife J.C., Naik G.V., Nnanna A.G.A., Kildishev A.V., Shalaev V.M., et al., Local Heating with Lithographically Fabricated Plasmonic Titanium Nitride Nanoparticles, *Nano Letters* 2013, 13(12): 6078–83.
- [19] Li W., Guler U., Kinsey N., Naik G.V., Boltasseva A., Guan J., et al., Refractory Plasmonics with Titanium Nitride: Broadband Metamaterial Absorber, *Advanced Materials* 2014, 26(47): 7959–65.
- [20] Guler U., Kildishev A.V., Boltasseva A., Shalaev V.M., Plasmonics on the slope of enlightenment: the role of transition metal nitrides, *Faraday Discussions* 2015, 178(0): 71–86.
- [21] Zhou N., Xu X., Hammack Aaron T., Stipe Barry C., Gao K., Scholz W., et al., Plasmonic near-field transducer for heat-assisted magnetic recording, *Nanophotonics* 2014, 3(3): 141–55.
- [22] Bauer T., *Thermophotovoltaics: Basic Principles and Critical Aspects of System Design*, Berlin, Germany: Springer-Verlag; 2011. 222 p.
- [23] Clavero C., Plasmon-induced hot-electron generation at nanoparticle/metal-oxide interfaces for photovoltaic and photocatalytic devices, *Nat Photon.* 2014, 8(2): 95–103.
- [24] Linic S., Christopher P., Ingram D.B., Plasmonic-metal nanostructures for efficient conversion of solar to chemical energy, *Nat Mater.* 2011, 10(12): 911–21.
- [25] Mukherjee S., Libisch F., Large N., Neumann O., Brown L.V., Cheng J., et al., Hot Electrons Do the Impossible: Plasmon-Induced Dissociation of H₂ on Au, *Nano Letters* 2012, 2013/01/09, 13(1): 240–7.
- [26] Boyd D.A., Greengard L., Brongersma M., El-Naggar M.Y., Goodwin D.G., Plasmon-Assisted Chemical Vapor Deposition, *Nano Letters*. 2006, 6(11): 2592–7.
- [27] Wakabayashi H., Saito Y., Takeuchi K., Mogami T., Kunio T., A dual-metal gate CMOS technology using nitrogen-concentration-controlled TiN_x film, *Electron Devices, IEEE Transactions on*. 2001, 48(10): 2363–9.

- [28] Dong S., Chen X., Gu L., Zhang L., Zhou X., Liu Z., et al., A biocompatible titanium nitride nanorods derived nanostructured electrode for biosensing and bioelectrochemical energy conversion, *Biosensors and Bioelectronics* 2011, 26(10): 4088–94.
- [29] Hyde G.K., McCullen S.D., Jeon S., Stewart S.M., Jeon H., Lobo E.G., et al., Atomic layer deposition and biocompatibility of titanium nitride nano-coatings on cellulose fiber substrates, *Biomedical Materials* 2009, 4(2): 025001.
- [30] Wisbey A., Gregson P.J., Tuke M., Application of PVD TiN coating to Co-Cr-Mo based surgical implants, *Biomaterials* 1987, 8(6): 477–80.
- [31] Li J., Gao L., Sun J., Zhang Q., Guo J., Yan D., Synthesis of Nanocrystalline Titanium Nitride Powders by Direct Nitridation of Titanium Oxide, *Journal of the American Ceramic Society* 2001, 84(12): 3045–7.
- [32] Saha N.C., Tompkins H.G., Titanium nitride oxidation chemistry: An xray photoelectron spectroscopy study, *Journal of Applied Physics* 1992, 72(7): 3072–9.
- [33] Jaque D., Martínez Maestro L., del Rosal B., Haro-Gonzalez P., Benayas A., Plaza J.L., et al., Nanoparticles for photothermal therapies, *Nanoscale* 2014, 6(16): 9494–530.
- [34] Loo C., Lin A., Hirsch L., Lee M.H., Barton J., Halas N., et al., Nanoshell-enabled photonics-based imaging and therapy of cancer, *Technol Cancer Res Treat.* 2004 Feb, 3(1): 33–40.
- [35] Hirsch L.R., Stafford R.J., Bankson J.A., Sershen S.R., Rivera B., Price R.E., et al., Nanoshell-mediated near-infrared thermal therapy of tumors under magnetic resonance guidance, *Proceedings of the National Academy of Sciences* 2003, 100(23): 13549–54.
- [36] Hirsch L.R., Jackson J.B., Lee A., Halas N.J., West J.L., A Whole Blood Immunoassay Using Gold Nanoshells, *Analytical Chemistry* 2003, 2003/05/01, 75(10): 2377–81.
- [37] Huang P., Lin J., Li W., Rong P., Wang Z., Wang S., et al., Biodegradable Gold Nanovesicles with an Ultrastrong Plasmonic Coupling Effect for Photoacoustic Imaging and Photothermal Therapy, *Angewandte Chemie International Edition* 2013, 52(52): 13958–64.
- [38] Goodman A.M., Cao Y., Urban C., Neumann O., Ayala-Orozco C., Knight M.W., et al., The Surprising in Vivo Instability of Near-IR-Absorbing Hollow Au–Ag Nanoshells, *ACS Nano*. 2014, 2014/04/22, 8(4): 3222–31.
- [39] Xie J., Lee S., Chen X., Nanoparticle-based theranostic agents, *Advanced Drug Delivery Reviews* 2010, 62(11): 1064–79.
- [40] Li Z., Huang P., Zhang X., Lin J., Yang S., Liu B., et al., RGD-Conjugated Dendrimer-Modified Gold Nanorods for in Vivo Tumor Targeting and Photothermal Therapy†, *Molecular Pharmaceutics* 2009, 2010/02/01, 7(1): 94–104.
- [41] Dasgupta S., Auth T., Gompper G., Shape and Orientation Matter for the Cellular Uptake of Nonspherical Particles, *Nano Letters* 2014, 2014/02/12, 14(2): 687–93.
- [42] Takada N., Sasaki T., Sasaki K., Synthesis of crystalline TiN and Si particles by laser ablation in liquid nitrogen, *Applied Physics A* 2008, 2008/12/01, 93(4): 833–6.
- [43] Yang X., Li C., Yang L., Yan Y., Qian Y., Reduction-Nitridation Synthesis of Titanium Nitride Nanocrystals, *Journal of the American Ceramic Society* 2003, 86(1): 206–8.
- [44] George P.P., Gedanken A., Makhlof S.-D., Genish I., Marciano A., Abu-Mukh R., Synthesis and characterization of titanium nitride, niobium nitride, and tantalum nitride nanocrystals via the RAPET (reaction under autogenic pressure at elevated temperature) technique; *Journal of Nanoparticle Research* 2009, 2009/05/01, 11(4): 995–1003.
- [45] Calka A., Formation of titanium and zirconium nitrides by mechanical alloying, *Applied Physics Letters* 1991, 59(13): 1568–9.
- [46] Kumar S., Murugan K., Chandrasekhar S.B., Hebalkar N., Krishna M., Satyanarayana B.S., et al., Synthesis and characterization of nano silicon and titanium nitride powders using atmospheric microwave plasma technique, *Journal of Chemical Sciences* 2012, 2012/05/01, 124(3): 557–63.
- [47] Dekker J.P., van der Put P.J., Veringa H.J., Schoonman J., Vapour-phase synthesis of titanium nitride powder, *Journal of Materials Chemistry* 1994, 4(5): 689–94.
- [48] Aghababazadeh R., Mirhabibi A.R., Rand B., Banijamali S., Pourasad J., Ghahari M., Synthesis and characterization of nanocrystalline titanium nitride powder from rutile and anatase as precursors, *Surface Science* 2007, 601(13): 2881–5.
- [49] Egerton R.F., Electron energy-loss spectroscopy in the TEM, *Reports on Progress in Physics* 2009, 72(1): 016502.
- [50] Reddy B.V., Khanna S.N., Structure and stability of Ti_nN_m clusters, *Physical Review B* 1996, 54(3): 2240–3.
- [51] Weir A., Westerhoff P., Fabricius L., Hristovski K., von Goetz N., Titanium Dioxide Nanoparticles in Food and Personal Care Products, *Environmental Science & Technology* 2012, 2012/02/21, 46(4): 2242–50.
- [52] Tompkins H.G., The initial stages of the oxidation of titanium nitride, *Journal of Applied Physics* 1992, 71(2): 980–3.
- [53] Bannister F.A., Osbornite, meteoric titanium nitride, *Mineralogical Magazine* 1941, 26: 36–44.
- [54] Stuart H.R., Hall D.G., Island size effects in nanoparticle-enhanced photodetectors, *Applied Physics Letters* 1998, 73(26): 3815–7.
- [55] Bohren C., Huffman D., *Absorption and Scattering of Light by Small Particles* (Wiley science paperback series): Wiley-VCH, 1998.